Acta Cryst. (1999). B**55**, 266–272

Cation distribution and crystal chemistry of $Y_3Al_{5-x}Ga_xO_{12}$ ($0 \leq x \leq 5$) garnet solid solutions

Akihiko Nakatsuka,*† Akira Yoshiasa and Takamitsu Yamanaka

Department of Earth and Space Science, Graduate School of Science, Osaka University, Toyonaka, Osaka 560-0043, Japan. E-mail: tuka@po.cc.yamaguchi-u.ac.jp

(*Received 6 February 1996; accepted 29 November 1998*)

Abstract

Five single crystals of $Y_3Al_{5-x}Ga_xO_{12}$ ($0 \leq x \leq 5$) garnet solid solutions with the compositions x = 0.0, 1.0, 2.0, 3.0 and 4.0 were synthesized using a flux method. The compositional dependence of the lattice constants of the garnet solid solutions shows a large deviation from Vegard's law. Investigation of the cation distributions of these garnets using single-crystal X-ray diffraction shows that Ga^{3+}, which is larger than Al^{3+}, preferentially occupies the tetrahedral (four-coordinate) site rather than the octahedral (six-coordinate) site. On the basis of the results obtained from structure refinements, geometric analyses of the polyhedral distortions were carried out. The results imply that the cation–cation repulsive force across the polyhedral shared edges decreases with increasing substitution of Ga^{3+}. Moreover, the proportion of covalent bonding in the cation–oxygen bonds was estimated from the bond strength; the results indicate that the covalency of the Ga—O bond is greater than that of the Al—O bond. The peculiar cation distributions observed in the $Y_3Al_{5-x}Ga_xO_{12}$ garnet solid solutions are most probably caused by the strong covalency of the Ga—O bond and also simultaneously induced by the need to decrease the cation–cation repulsive force. Crystal data: cubic, $Ia\bar{3}d$, Z = 8, Mo $K\alpha$, λ = 0.71069 Å; at x = 0.0 (triyttrium pentaaluminium dodecaoxide): a_0 = 12.0062 (5) Å, V = 1730.7 (2) Å^3, D_x = 4.56 Mg m^{-3}, M_r = 593.613, μ = 21.21 mm^{-1}, $F(000)$ = 2224, R = 0.029 for 294 reflections; at x = 1.0 (triyttrium tetraaluminium gallium dodecaoxide): a_0 = 12.0432 (7) Å, V = 1746.7 (3) Å^3, D_x = 4.84 Mg m^{-3}, M_r = 636.351, μ = 24.09 mm^{-1}, $F(000)$ = 2368, R = 0.022 for 124 reflections; at x = 2.0 (triyttrium trialuminium digallium dodecaoxide): a_0 = 12.0926 (9) Å, V = 1768.3 (4) Å^3, D_x = 5.10 Mg m^{-3}, M_r = 679.089, μ = 26.85 mm^{-1}, $F(000)$ = 2512, R = 0.018 for 144 reflections; at x = 3.0 (triyttrium dialuminium trigallium dodecaoxide): a_0 = 12.1552 (6) Å, V = 1795.9 (3) Å^3, D_x = 5.34 Mg m^{-3}, M_r = 721.827, μ = 29.43 mm^{-1}, $F(000)$ = 2656, R = 0.018 for 184 reflections; at x = 4.0 (triyttrium aluminium tetragallium dodecaoxide): a_0 = 12.2123 (8) Å, V = 1821.3 (4) Å^3, D_x = 5.58 Mg m^{-3}, M_r = 764.565, μ = 31.97 mm^{-1}, $F(000)$ = 2800, R = 0.014 for 159 reflections.

1. Introduction

The crystal structures and chemistry of garnets have been intensively investigated by many researchers (*e.g.* Zemann, 1962; Euler & Bruce, 1965; Geller, 1967; Novak & Gibbs, 1971; Meagher, 1975; Takéuchi *et al.*, 1982; Pavese *et al.*, 1995) in the seventy years since the crystal structure was first determined by Menzer (1926). In particular, Novak & Gibbs (1971) systematically discussed the crystal chemistry of silicate garnets on the basis of variations of their interatomic distances and angles, lattice constants *etc.* They proposed a linear relationship between the lattice constants and the mean cation size on the dodecahedral (eight-coordinate) and the octahedral sites in silicate garnets. Their results suggest that structural variations of garnets are mainly induced by variation of the cation sizes. In the $Y_3Fe_{5-x}Ga_xO_{12}$ (Y–Fe–Ga) system, however, our previous study (Nakatsuka *et al.*, 1995) pointed out that the structural variations (cation distribution, interatomic distances, lattice constants *etc.*) caused by cation substitution are closely related to the cation–cation repulsive force across the polyhedral shared edges. In practice, in most of the garnet solid solutions the compositional dependence of the lattice constants deviates from the values expected from Vegard's law.

Marezio *et al.* (1968) studied the site preference of Ga^{3+} in the $Y_3Al_{5-x}Ga_xO_{12}$ (Y–Al–Ga) system by single-crystal X-ray diffraction. In this system, Al^{3+} is substituted by the larger Ga^{3+} (Shannon, 1976). Marezio *et al.* (1968) reported that Ga^{3+} preferentially occupies the tetrahedral site rather than the octahedral site. This cation distribution can not be explained from the viewpoint of cation size because in this system the larger cations (Ga^{3+}) preferentially occupy the smaller (tetrahedral) site and the smaller cations (Al^{3+}) preferentially occupy the larger (octahedral) site. Moreover, although the garnets in this system have such peculiar cation distributions, the compositional dependence of the lattice constants obtained by Marezio *et al.* (1968) follows Vegard's law well. However, they gave no

---

† Present address: Department of Advanced Materials Science and Engineering, Faculty of Engineering, Yamaguchi University, Ube, Yamaguchi 755-8611, Japan.

Table 1. *Experimental details*

	$x = 0.0$	$x = 1.0$	$x = 2.0$	$x = 3.0$	$x = 4.0$
Crystal data					
Chemical formula	$Y_3Al_5O_{12}$	$Y_3Al_4GaO_{12}$	$Y_3Al_3Ga_2O_{12}$	$Y_3Al_2Ga_3O_{12}$	$Y_3AlGa_4O_{12}$
Chemical formula weight	593.613	636.351	679.089	721.827	764.565
Cell setting	Cubic	Cubic	Cubic	Cubic	Cubic
Space group	$Ia\bar{3}d$	$Ia\bar{3}d$	$Ia\bar{3}d$	$Ia\bar{3}d$	$Ia\bar{3}d$
a_0 (Å)	12.0062 (5)	12.0432 (7)	12.0926 (9)	12.1552 (6)	12.2123 (8)
V (Å^3)	1730.7 (2)	1746.7 (3)	1768.3 (4)	1795.9 (3)	1821.3 (4)
Z	8	8	8	8	8
D_x (Mg m^{-3})	4.56	4.84	5.10	5.34	5.58
μ (mm^{-1})	21.21	24.09	26.85	29.43	31.97
Temperature (K)	296	296	296	296	296
Crystal radius (mm)	0.095	0.055	0.105	0.070	0.073
Data collection					
No. of measured reflections	3294	3309	3359	3400	3074
No. of observed independent reflections [$\lvert F_o \rvert > 3\sigma(\lvert F_o \rvert)$]	294	124	144	184	159
$R_{\rm int}$	0.019	0.024	0.015	0.016	0.010
Refinement					
Refinement on	F	F	F	F	F
R	0.029	0.022	0.018	0.018	0.014
wR	0.026	0.016	0.017	0.013	0.009
No. of reflections used in refinement	294	124	144	184	159

explanation for the peculiar cation distribution and the variation of the lattice constants in this system. Factors other than the effect of cation size must determine the cation distribution in this system. Cation distributions in crystals should also be influenced by the effects of the cation–cation repulsive forces and the bonding nature of the cation–oxygen bonds (Nakatsuka *et al.*, 1995).

In this study, the reason for the peculiar cation distribution in the Y–Al–Ga system is examined by single-crystal X-ray diffraction. Special attention is paid to the bonding nature of the cation–oxygen bonds and the effect of the cation–cation repulsive force in connection with the our previous study of the Y–Fe–Ga system.

2. Experimental

2.1. *Specimen preparation and characterization*

The single crystals of $Y_3Al_{5-x}Ga_xO_{12}$ garnet solid solutions used in this study were grown using a PbF_2 flux. Special grade reagents (99.99%) of Y_2O_3, α-Al_2O_3 and Ga_2O_3 were used as starting materials and mixed together in molar ratios Y_2O_3:α-Al_2O_3:Ga_2O_3 = 3:$(5 - x)$:x. Each mixture of the starting materials and PbF_2 flux was placed in a 30 cm^3 platinum crucible, heated slowly to 1473 K, cooled down at a rate of 5 K h^{-1} to 1023 K and then cooled naturally in the furnace from 1023 K to room temperature (296 K) under atmospheric conditions. The temperature fluctuation in the furnace was kept within ±1 K. The composition and homogeneity of the crystals obtained were examined using a JEOL JCMA-733 electron-microprobe analyzer. The results of the chemical analyses ascertained the homogeneity of the crystals and little compositional fluctuation was observed. Five crystals, with $x = 0.0$, 1.0, 2.0, 3.0 and 4.0, were obtained.

2.2. *X-ray intensity measurements*

For intensity measurements each single crystal was ground into a sphere 0.11–0.21 mm in diameter. Prior to intensity measurements, the systematic absences (hkl reflections are present only with $h + k + l = 2n$; $0kl$ only with $k, l = 2n$; hhl only with $2h + l = 4n$; $h00$ only with $h = 4n$) were examined using Weissenberg photographs at room temperature. All results were consistent with space-group symmetry $Ia\bar{3}d$.

The intensity data and lattice constants were measured using a Rigaku AFC-6 four-circle diffractometer at room temperature. Mo $K\alpha$ radiation (λ = 0.71069 Å) obtained from a rotating-anode X-ray generator (50 kV, 200 mA) and monochromated by pyrolytic graphite was used. The lattice constants were refined by the least-squares method using the 2θ values of 25 reflections in the range $45 \leq 2\theta \leq 50°$. The same set of 25 reflections was used for all five crystals. A silicon single crystal was used as a standard material for the lattice-constant determinations. Reflection intensities in the range $2 \leq 2\theta \leq 120°$ were measured in the ω–2θ scan mode. Intensity data were corrected for Lorentz and polarization factors and for absorption assuming a sphere (μr = 1.33–2.82 for Mo $K\alpha$ radiation). For each specimen, 3074–3400 reflections were measured. 124–294 independent reflections with $|F_o| > 3\sigma(|F_o|)$ after averaging equivalent reflections were used for the refinements. Coincidence factors for the equivalent reflections ($R_{\rm int}$ in Table 1) were 0.010–0.024.

3. Refinements

The structure refinements were carried out using the full-matrix least-squares program *RFINE*2 (Finger, 1969). The initial values for the parameters used in the present study were those of $Y_3Fe_5O_{12}$ given by Nakatsuka *et al.* (1995). Atomic scattering factors for neutral atoms and correction terms for anomalous dispersion were taken from *International Tables for X-ray Crystallography* (1974, Vol. IV).

From consideration of the effective ionic radii (Shannon, 1976), we may consider that Y^{3+} occupies only the dodecahedral site, and Al^{3+} and Ga^{3+} occupy both the octahedral and the tetrahedral sites. The occupancy of the dodecahedral site was therefore fixed at unity, and the occupancies of the octahedral and the tetrahedral sites were constrained to maintain the chemical composition of each specimen. Consequently, the only variable occupancy parameter was that of Ga^{3+} on the octahedral site. During the least-squares refinements a correction for isotropic extinction was applied. After several cycles of refinements the displacement parameters were converted to an anisotropic model.

The final R and wR factors for each specimen were 0.014–0.029 and 0.009–0.026, respectively (Table 1).† Crystallographic data and details of the structure refinements are summarized in Table 1. The refined positional, occupancy and equivalent isotropic displacement parameters are listed in Table 2. Selected interatomic distances are given in Table 3.‡

Table 2. *Fractional atomic coordinates and equivalent isotropic displacement parameters (Å²)*

The sites ($\frac{1}{8}$,0,$\frac{1}{4}$), (0,0,0) and ($\frac{3}{8}$,0,$\frac{1}{4}$) are the dodecahedral, the octahedral and the tetrahedral sites, respectively.

$$B_{\rm eq} = (4/3)\Sigma_i\Sigma_j\beta^{ij}\mathbf{a}_i.\mathbf{a}_j.$$

	x	y	z	$B_{\rm eq}$
x = 0.0				
Y	1/8	0	1/4	0.32
Al1	0	0	0	0.37
Al2	3/8	0	1/4	0.39
O	−0.0318 (3)	0.0511 (3)	0.1498 (3)	0.31
x = 1.0				
Y	1/8	0	1/4	0.16
Al1/Ga1†	0	0	0	0.40
Al2/Ga2‡	3/8	0	1/4	0.93
O	−0.0293 (4)	0.0497 (4)	0.1498 (4)	0.69
x = 2.0				
Y	1/8	0	1/4	0.19
Al1/Ga1§	0	0	0	0.58
Al2/Ga2¶	3/8	0	1/4	1.20
O	−0.0299 (4)	0.0527 (4)	0.1498 (4)	0.54
x = 3.0				
Y	1/8	0	1/4	0.30
Al1/Ga1††	0	0	0	0.47
Al2/Ga2‡‡	3/8	0	1/4	0.68
O	−0.0278 (3)	0.0523 (3)	0.1495 (3)	0.54
x = 4.0				
Y	1/8	0	1/4	0.34
Al1/Ga1§§	0	0	0	0.43
Al2/Ga2¶¶	3/8	0	1/4	0.71
O	−0.0279 (3)	0.0540 (2)	0.1498 (3)	0.61

† Site occupancy Al:Ga 0.927:0.073 (8). ‡ Site occupancy Al:Ga 0.716:0.284. § Site occupancy Al:Ga 0.802:0.198 (8). ¶ Site occupancy Al:Ga 0.465:0.535. †† Site occupancy Al:Ga 0.591:0.409 (6). ‡‡ Site occupancy Al:Ga 0.273:0.727. §§ Site occupancy Al:Ga 0.354:0.646 (5). ¶¶ Site occupancy Al:Ga 0.097:0.903.

4. Results and discussion

The cubic garnet structure belongs to space group $Ia\bar{3}d$ with cations at special positions (on 24*c*, 16*a* and 24*d* sites) and oxygen anions at general positions (on a 96*h* site). Each tetrahedron and octahedron share edges with two and six triangular dodecahedra, respectively. Each triangular dodecahedron shares edges with two tetrahedra, four octahedra and four other triangular dodecahedra. The tetrahedra and octahedra are linked to each other by sharing all corners (Fig. 1).

4.1. *Cation distribution*

The structural formula in the $Y_3Al_{5-x}Ga_xO_{12}$ system can be generally expressed as $\{Y\}_3[Al_{1-p}Ga_p]_2$-$(Al_{(3-x+2p)/3}Ga_{(x-2p)/3})_3O_{12}$, where { }, [ ], ( ), p and x refer to the dodecahedral site, the octahedral site, the tetrahedral site, the occupancy parameter of Ga^{3+} on the octahedral site and the composition (Ga^{3+} content) of the specimen, respectively. The fractional parameter $f_{\rm Ga}$ corresponding to the degree of Ga^{3+} preference for the tetrahedral site is defined by $f_{\rm Ga} = 1 - (2p/x)$. Ga^{3+} and Al^{3+} are distributed without any site preference on both the tetrahedral and the octahedral sites when $f_{\rm Ga}$ is 0.6 ($p = 0.2x$), because the cation ratio between the octahedral and the tetrahedral sites is 2:3. The $f_{\rm Ga}$ values for

---

† $R = \sum(||F_o| - |F_c||)/\sum|F_o|$ and $wR = [\sum w(|F_o| - |F_c|)^2/\sum w|F_o|^2]^{1/2}$ with weighting scheme $w = 1/\sigma^2(|F_o|)$.

‡ Supplementary data for this paper are available from the IUCr electronic archives (Reference: OH0057). Services for accessing these data are described at the back of the journal.

the compositions studied here are given in Table 4 together with those of Marezio *et al.* (1968). The present $f_{\rm Ga}$ values are much larger than 0.6 for all the compositions, indicating that $\rm Ga^{3+}$ significantly prefers the tetrahedral site, contrary to the effect of cation size ($r_{\rm Ga} > r_{\rm Al}$; Shannon, 1976). The selectivity of $\rm Ga^{3+}$ for the tetrahedral site occurs despite increasing substitution of $\rm Ga^{3+}$. These results agree with those of Marezio *et al.* (1968).

4.2. *Polyhedral distortion and lattice constants*

The interatomic distances d_i (i = 4, 6, 8, 80, 48, 68, 88, 41, 61, 81, 82, 83) are labelled in Fig. 1. Fig. 2 shows the variation of the cation–oxygen distances with the composition (x). With increasing $\rm Ga^{3+}$ content, d_4 increases twice as fast as d_6 ($\Delta d_4/\Delta x{:}\Delta d_6/\Delta x \simeq 1.9{:}1$). This variation of the cation–oxygen distances results from the displacement of oxygen anions caused by the preference of the larger cation ($\rm Ga^{3+}$) for the tetrahedral site. This mode of displacement of oxygen anions, caused by structural geometric restrictions, is consistent with the results of Nakatsuka *et al.* (1995).

Fig. 3 shows the variation of the ratio $\rm (O{-}O)_{shared}/(O{-}O)_{unshared}$ in the polyhedra with the composition (x). In the triangular dodecahedron, the ratio of the length of the edge (d_{88}) shared with an adjacent dodecahedron to the shortest length (d_{81}) of the three symmetry-nonequivalent unshared edges (d_{81}, d_{82} and d_{83}) is plotted. With increasing $\rm Ga^{3+}$ content, the polyhedral shared edges are shortened compared with the polyhedral unshared edges. This relationship between the shared and the unshared edges is caused by the displacement of the oxygen anions described above. The results shown in Fig. 3 imply that the shielding effect of the anions forming the polyhedral shared edges, which relaxes the repulsive force between the cations across the shared edges, increases with increasing $\rm Ga^{3+}$ content [refer to Tossell & Gibbs (1977) and Hill *et al.* (1983) for a discussion of this shielding effect]. That is, the cation–cation repulsive force across the shared edges will decrease with increasing $\rm Ga^{3+}$ content. The decrease in

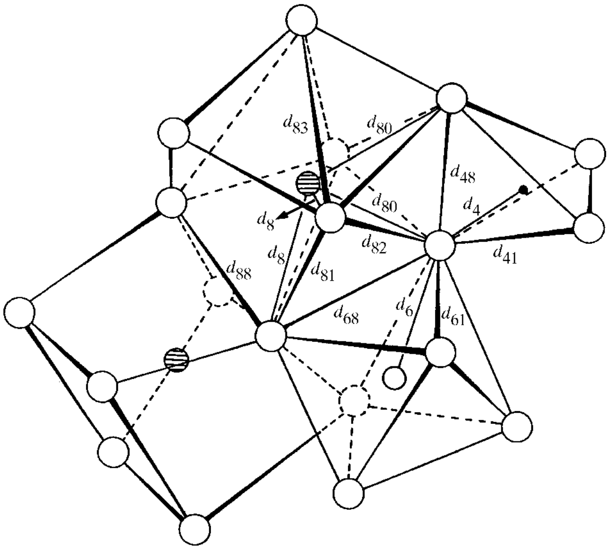

Fig. 1. Schematic O-atom coordination polyhedra in the garnet structure (after Novak & Gibbs, 1971). Large open circles, hatched circles, small open circles and small filled circles represent O atoms, the dodecahedral-site cations, the octahedral-site cations and the tetrahedral-site cations, respectively.

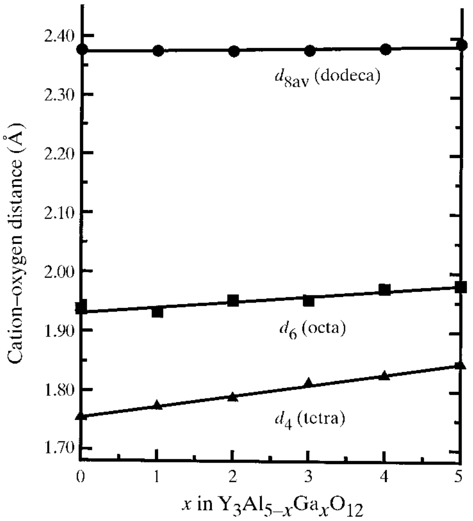

Fig. 2. The compositional dependence of the cation–oxygen distances. d_4 (filled triangles) and d_6 (filled squares) are the cation–oxygen distances for the tetrahedral and the octahedral sites, respectively, and $d_{8\rm av}$ (filled circles) is the average of the two symmetry-nonequivalent cation–oxygen distances (d_8 and d_{80}) for the dodecahedral site. Data for x = 5.0 are from Nakatsuka *et al.* (1995).

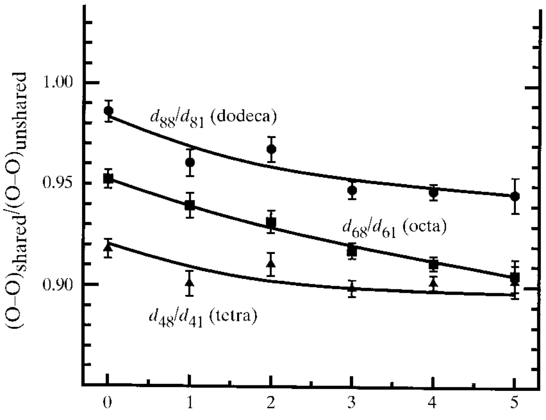

Fig. 3. Variation of the ratio $\rm (O{-}O)_{shared}/(O{-}O)_{unshared}$ in each polyhedron plotted against the composition (x). Filled circles, filled squares and filled triangles represent the ratio $\rm (O{-}O)_{shared}/(O{-}O)_{unshared}$ on the dodecahedral (d_{88}/d_{81}), the octahedral (d_{68}/d_{61}) and the tetrahedral sites (d_{48}/d_{41}), respectively. The data for x = 5.0 were calculated from the lengths of the polyhedral shared and unshared edges given by Nakatsuka *et al.* (1995).

Table 3. *Selected interatomic distances (Å)*

(*a*) Cation–oxygen interatomic distances

Composition (*x*)	d_4	d_6	d_{80}	d_8	d_{8av}†
0.0	1.754 (4)	1.938 (4)	2.317 (4)	2.437 (4)	2.377 (4)
1.0	1.773 (5)	1.933 (5)	2.296 (5)	2.456 (5)	2.376 (5)
2.0	1.788 (5)	1.953 (5)	2.321 (5)	2.432 (4)	2.376 (5)
3.0	1.814 (3)	1.955 (4)	2.312 (3)	2.445 (3)	2.379 (3)
4.0	1.827 (3)	1.974 (3)	2.327 (3)	2.437 (3)	2.382 (3)

(*b*) Polyhedral shared edges

Composition (*x*)	d_{48}	d_{68}	d_{88}
0.0	2.702 (7)	2.673 (7)	2.859 (8)
1.0	2.695 (10)	2.648 (9)	2.856 (10)
2.0	2.739 (9)	2.664 (8)	2.831 (9)
3.0	2.754 (7)	2.644 (6)	2.826 (7)
4.0	2.779 (6)	2.660 (5)	2.810 (6)

(*c*) Polyhedral unshared edges

Composition (*x*)	d_{41}	d_{61}	d_{81}
0.0	2.943 (7)	2.806 (7)	2.900 (8)
1.0	2.990 (9)	2.817 (9)	2.972 (10)
2.0	3.006 (8)	2.858 (8)	2.925 (9)
3.0	3.062 (6)	2.880 (6)	2.981 (7)
4.0	3.081 (5)	2.918 (5)	2.967 (6)

† d_{8av} is the average of d_8 and d_{80}.

the cation–cation repulsive force should result in a closer approach of the cations.

Fig. 4 shows the variation of the lattice constants (a_0) with the composition (x), together with the results of Marezio *et al.* (1968). In the cubic garnet structure, the variation of the lattice constants directly reflects that of the cation–cation distances because all the cations are located at special positions. The compositional dependence of the lattice constants in the present study shows a large deviation from Vegard's law; the lattice constants obtained in the present study are smaller than those expected from Vegard's law for the whole composition range. This implies that the decrease in the cation–cation repulsive force allows shorter cation–cation distances than expected.

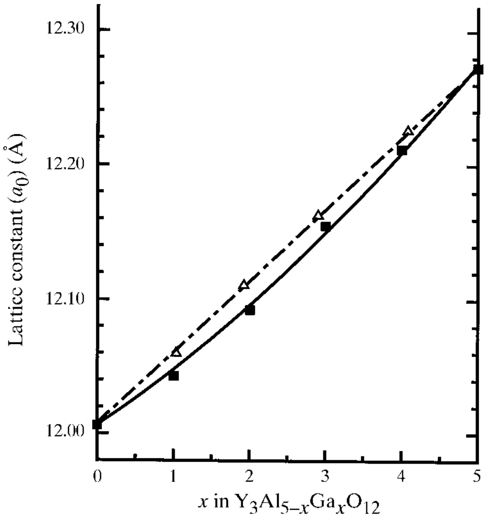

Fig. 4. The compositional dependence of the lattice constants (a_0). The dashed-and-dotted line shows the variation expected from Vegard's law. Filled squares: this study; open triangles: Marezio *et al.* (1968). The lattice constants obtained in this study fluctuate below the line expected from Vegard's law. Data for $x = 5.0$ are from Nakatsuka *et al.* (1995).

As described above, the cation-distribution results of Marezio *et al.* (1968) and the present study indicate the strong preference of Ga^{3+} for the tetrahedral site. However, the lattice constants given by Marezio *et al.* (1968) follow Vegard's law exactly (Fig. 4), although Vegard's law is realized only in the case of a random cation distribution.

4.3. *Covalency of the cation–oxygen bonds*

The bond-valence sums around the O atoms calculated using the parameters given by Brown (1981) are 1.98, 2.02, 2.01, 2.01 and 2.00 for the compositions x = 0.0, 1.0, 2.0, 3.0 and 4.0, respectively. The values show that the present results for the site occupancies are reliable.

The proportion of covalent bonding in the cation–oxygen bonds was estimated using the equations proposed by Brown & Shannon (1973),

$$f'_c = as^M$$
$$q = 100f'_c/s = 100as^{M-1},$$

where f'_c, s and q are the covalency of the cation–oxygen bonds (v.u.), the bond strength (v.u.) and the proportion of covalent bonding (%), respectively, and a and M are constants for isoelectric ions. Fig. 5 shows the compositional dependence of the q value. It is reasonable that the q values for the tetrahedral site are greater than those for the octahedral site. With increasing Ga^{3+} content, the q values on the tetrahedral and the octahedral sites increase. This indicates that the covalency of the Ga—O bond is greater than that of the Al—O bond. This is also confirmed for other compounds, *e.g.* GaN, GaP, GaAs, AlN, AlP and AlAs. According to García & Cohen (1993), who calculated the ionicity for A^NB^{8-N} compounds from the valence charge density, GaN, GaP and GaAs have stronger covalency than AlN, AlP and AlAs, respectively. Their results are concordant with the electronegativities given by Allred & Rochow (1958), Pauling (1960) and Sanderson (1967). Thus, we may generally consider that the electronegativity of Ga (χ_{Ga}) is greater than that of Al (χ_{Al}).

From consideration of the bonding nature ($\chi_{Ga} > \chi_{Al}$), the peculiar preference of Ga^{3+} for the tetrahedral site should cause a more remarkable increase in the q values with increasing Ga^{3+} content for the tetrahedral site than for the octahedral site. However, as shown in Fig. 5, the rate of increase in the q values for the octahedral site with increasing Ga^{3+} content is approximately twice that for the tetrahedral site. This can be explained by the displacement of oxygen anions as a result of the substitution of cations with different sizes. As described above, with increasing Ga^{3+} content, d_4 increases more remarkably than d_6. As a result of the displacement of oxygen anions, caused by the structural geometric restrictions, the oxygen electron cloud will be attracted toward the octahedral cation more than toward the tetrahedral cation as the Ga^{3+} content increases; consequently, the oxygen electron cloud will move away from the tetrahedral cation more than from the octahedral cation.

4.4. *Interpretation of the cation distribution*

In general, the cation distribution in crystals containing cations without ligand-field effects can be mainly attributed to the cation sizes and the nature of the bonding. The strong covalency of the Ga—O bond can be considered to be one of the reasons for the strong Ga^{3+} preference for the tetrahedral site in the Y–Al–Ga system, causing the cation distribution to contradict the effect of cation size. Other factors must also be considered, however, as seen in the spinel $MgAl_2O_4$. The cation distribution in $MgAl_2O_4$ spinel is the normal type, contrary to the effects of both the cation size ($r_{Mg} > r_{Al}$; Shannon, 1976) and the electronegativity ($\chi_{Al} > \chi_{Mg}$; Allred & Rochow, 1958; Pauling, 1960; Sanderson, 1967), *i.e.*, Mg^{2+} and Al^{3+} occupy the tetrahedral and the octahedral sites, respectively. This indicates that the factors that determine the site preference of cations in crystals are not only the cation size and electronegativity. Thus, as for the cation distribution in the Y–Al–Ga system, other factors should be considered as well.

Table 4. *The fractional parameter* f_{Ga}

Marezio *et al.* (1968)		This work	
Composition (x)	f_{Ga}	Composition (x)	f_{Ga}
1.03	0.84 (3)	1.0	0.853 (16)
1.92	0.77 (2)	2.0	0.802 (8)
2.90	0.68 (1)	3.0	0.727 (4)
4.08	0.63 (1)	4.0	0.677 (3)

The effect of the cation–cation repulsive force should be considered as another factor determining the cation distribution in the Y–Al–Ga system. Nakatsuka *et al.* (1995) indicated that the preferential occupation of the octahedral site by larger cations in the Y–Fe–Ga system results in an increase in the ratio $(O\text{–}O)_{shared}/(O\text{–}O)_{unshared}$. Considering their results and the tendency seen in Fig. 3, if Ga^{3+} preferentially occupied the octahedral site according to the cation size, the ratio d_{88}/d_{81}, 0.986 (5), at the composition x = 0.0 (Fig. 3) would exceed 1.0 and consequently the crystal structure would be destabilized because of the remarkable enhancement of the cation–cation repulsive force as a result of the extreme decrease in the shielding effect.

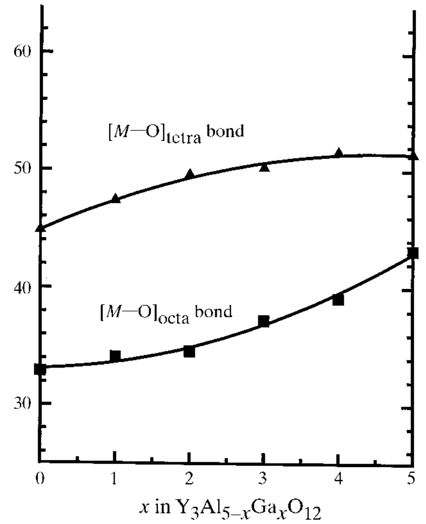

Fig. 5. The compositional dependence of the proportion (q) of covalent bonding in the cation–oxygen bonds at the octahedral and the tetrahedral sites. Filled triangles and filled squares represent the q values of the cation–oxygen bonds on the tetrahedral ($[M\text{—O}]_{tetra}$) and the octahedral sites ($[M\text{—O}]_{octa}$), respectively. The q values for x = 5.0 were calculated using the bond lengths given by Nakatsuka *et al.* (1995).

Hence, we believe that the decrease in the ratio $(O–O)_{shared}/(O–O)_{unshared}$ owing to the selectivity of Ga^{3+} for the tetrahedral site is indispensable for stabilizing the crystal structure by decreasing the cation–cation repulsive force, *i.e.*, by enhancing the shielding effect. Thus, the peculiar cation distribution in the Y–Al–Ga system is most probably a consequence of the need to decrease the cation–cation repulsive force as well as the effect of electronegativity. At the present, however, it is not easy to know whether the effect of electronegativity or the need to decrease the cation–cation repulsive force is the dominating factor in determining the peculiar cation distribution in this system.

5. Concluding remarks

In this paper, the cation distributions in the $Y_3Al_{5-x}Ga_xO_{12}$ garnet solid solutions were investigated by single-crystal X-ray diffraction analyses. Contrary to the effect of cation size, Ga^{3+} preferentially occupies the tetrahedral site over the octahedral site. From an estimate of the proportion of covalent bonding based on bond strength, we conclude that one of the main reasons for this peculiar cation distribution is the stronger covalency of the Ga—O bond compared with the Al—O bond. Moreover, the results of the geometric analyses of polyhedral distortion imply that the preference of Ga^{3+} for the tetrahedral site brings about a decrease in the cation–cation repulsive force across the polyhedral shared edges with increasing Ga^{3+} content as a result of structural geometric restrictions. In other words, the selectivity of Ga^{3+} for the tetrahedral site is indispensable in decreasing the cation–cation repulsive force. The lattice constants (*i.e.* the cation–cation distances) are smaller than expected from Vegard's law, which supports the relaxation of the cation–cation repulsive force. Therefore, the peculiar cation distribution in the Y–Al–Ga system is a consequence not only of the strong covalency of the Ga—O bond but also of the need to decrease the cation–cation repulsive force. Hence, we believe that the peculiar cation distribution in this system keeps the cation–cation repulsive force to a minimum, which further stabilizes the crystal structure.

The authors would like to thank Drs O. Ohtaka and T. Nagai of Osaka University and Dr M. Ohkawa of Hiroshima University for valuable discussions and useful information. All computations were carried out at the Crystallographic Research Center, Institute for Protein Research, Osaka University, Japan.

References

Allred, A. L. & Rochow, E. G. (1958). *J. Inorg. Nucl. Chem.* **5**, 264–268.

Brown, I. D. (1981). *Structure and Bonding in Crystals*, Vol. II, edited by M. O'Keeffe and A. Navrotsky, pp. 1–30. New York: Academic Press.

Brown, I. D. & Shannon, R. D. (1973). *Acta Cryst.* A**29**, 266–282.

Euler, F. & Bruce, J. A. (1965). *Acta Cryst.* **19**, 971–978.

Finger, L. W. (1969). *Carnegie Inst. Washington Yearb.* **67**, 216–217.

García, A. & Cohen, M. L. (1993). *Phys. Rev. B*, **47**, 4215–4220.

Geller, S. (1967). *Z. Kristallogr.* **125**, 1–47.

Hill, R. J., Newton, M. D. & Gibbs, G. V. (1983). *J. Solid State Chem.* **47**, 185–200.

Marezio, M., Remeika, J. P. & Dernier, P. D. (1968). *Acta Cryst.* B**24**, 1670–1674.

Meagher, E. P. (1975). *Am. Mineral.* **60**, 218–228.

Menzer, G. (1926). *Z. Kristallogr.* **63**, 157–158.

Nakatsuka, A., Yoshiasa, A. & Takeno, S. (1995). *Acta Cryst.* B**51**, 737–745.

Novak, G. A. & Gibbs, G. V. (1971). *Am. Mineral.* **56**, 791–825.

Pauling, L. (1960). *The Nature of the Chemical Bond*, 3rd ed., p. 93. Ithaca: Cornell University Press.

Pavese, A., Artioli, G. & Prencipe, M. (1995). *Am. Mineral.* **80**, 457–464.

Sanderson, R. T. (1967). *Inorganic Chemistry*, pp. 72–76. New York: Van Nostrand-Reinhold.

Shannon, R. D. (1976). *Acta Cryst.* A**32**, 751–767.

Takéuchi, Y., Haga, N., Umizu, S. & Sato, G. (1982). *Z. Kristallogr.* **158**, 53–99.

Tossell, J. A. & Gibbs, G. V. (1977). *Phys. Chem. Mineral.* **2**, 21–57.

Zemann, J. (1962). *Beitr. Mineral. Petrogr.* **8**, 180–188.